Accelerated Publication

THE JOURNAL OF BIOLOGICAL CHEMISTRY
Vol. 277, No. 35, Issue of August 30, pp. 31279–31282, 2002
© 2002 by The American Society for Biochemistry and Molecular Biology, Inc.
Printed in U.S.A.

Mutant Products of the *NF2* Tumor Suppressor Gene Are Degraded by the Ubiquitin-Proteasome Pathway*

Received for publication, March 4, 2002,
and in revised form, July 17, 2002
Published, JBC Papers in Press, July 18, 2002,
DOI 10.1074/jbc.C200125200

Alexis Gautreau‡§, Jan Manent¶, Bruno Fievet‡, Daniel Louvard‡, Marco Giovannini¶, and Monique Arpin‡‖

From the ‡UMR144 CNRS/Institut Curie, 26 rue d'Ulm, 75248 Paris Cedex 05, France and ¶INSERM U434/CEPH, 27 rue Juliette Dodu, 75010 Paris, France

Neurofibromatosis type 2 (NF2), a syndrome associated with multiple tumors of the nervous system, mostly schwannomas, is caused by mutations in the *NF2* tumor suppressor gene that encodes schwannomin (Sch). Here we examined *NF2* pathogenetic mutations that result in misfolding of the FERM domain. We found that these mutant forms of Sch were efficiently degraded by the ubiquitin-proteasome pathway. In transfected cells, SchΔF118 was 3-fold more efficiently degraded than the related molecule ezrin bearing the equivalent mutation. In heterozygous *Nf2* knock-out mouse fibroblasts, endogenous mutant SchΔ81–121, but not wild type Sch, was also degraded by proteasomes. We further show that this degradation pathway is functional in primary Schwann cells. We analyzed SchΔ39–121 expressed in a transgenic mouse model of NF2 and found that SchΔ39–121, but not the endogenous wild type Sch, was unstable due to proteasome-mediated degradation. Altogether these results suggest that degradation of mutant Sch mediated by the ubiquitin-proteasome pathway is a physiopathological pathway contributing to the loss of Sch function in NF2 patients.

Neurofibromatosis type 2 (NF2)[1] is a dominantly inherited disorder characterized by the predisposition to develop multiple nervous system tumors, in particular schwannomas. Tumor development in NF2 patients is in accordance with Knudson's two-hit hypothesis for tumor suppressor genes. As NF2 patients inherit one mutant *NF2* allele, a second hit in the remaining wild type allele is sufficient to induce tumorigenesis. The two *NF2* alleles are also inactivated in the majority of sporadic schwannomas (1).

The *NF2* tumor suppressor gene product, Schwannomin (Sch), also known as merlin, displays 45% identity with ERM proteins, which are cytoskeletal linkers between cortical actin filaments and the plasma membrane (2, 3). Like ERM proteins, Sch has an amino-terminal FERM domain and a carboxyl-terminal domain that associate in an intramolecular manner to form closed monomers and in an intermolecular manner to form oligomers (4–6). The FERM domain of Sch binds to the plasma membrane and to filamentous actin (7, 8). Sch regulates cell adhesion and motility (9, 10) and mediates contact inhibition (11).

In human tumors, levels of mutant Sch are consistently below limits of detection although *NF2* mutant alleles were detected at the mRNA level (12–15). Therefore, we reasoned that mutant schwannomin might be degraded quickly. To examine this hypothesis, we studied the stability of mutant schwannomin in transfected cells or in primary cultures derived from mouse models developed to examine the pathogenesis of NF2 (16, 17). We focused on pathogenetic mutations in the conserved FERM domain of Sch. The deletion of the phenylalanine 118 codon in exon 3 has been described in two unrelated families affected by NF2 as well as in a sporadic meningioma (Ref. 12 and references therein). Mutations that lead to the skipping of exon 3 (SchΔ81–121) or exons 2–3 (SchΔ39–121) have been observed in the germ line or in the tumors of the NF2 patients (12, 18, 19). These mutations impair the proper folding of the schwannomin FERM domain (7). Here we report that these mutations destabilized the proteins and that these mutant proteins are efficiently degraded by the ubiquitin-proteasome pathway. Furthermore, degradation of mutant Sch occurred at endogenous level of expression and in Schwann cells, highlighting its relevance for NF2 pathogenesis.

MATERIALS AND METHODS

Cell Cultures—LLC-PK1 cells were cultured in DMEM containing 10% FBS and maintained at 37 °C in 10% CO_2. Primary fibroblasts were isolated from $Nf2^{KO3/+}$ embryos at 12.5 days of gestation using a standard procedure (20). For the establishment of primary mouse Schwann cell culture, sciatic nerves from 6-week-old transgenic P0-SchΔ39–121 mice or their wild type littermates (FVB/N strain) were dissected under sterile conditions and incubated for 7 days at 37 °C in 7.5% CO_2 in pretreatment medium containing DMEM with 4500 mg/liter glucose (Invitrogen), 10% FBS, 50 μg/ml gentamicin, 2 μM forskolin, and 10 ng/ml human recombinant heregulin-1β (R&D Systems) with fresh medium every 2 days. Nerves were then dissociated by incubation for 3 h in Leibowitz medium (L15) containing 0.5 mg/ml collagenase type I (Invitrogen) and 2.5 mg/ml dispase II (Roche Molecular Biochemicals) at 37 °C; triturated with a Pasteur pipette; resuspended in N-2 serum-free culture medium (21) supplemented with 50 μg/ml gentamicin, 2 μM forskolin, and 10 ng/ml heregulin-1β; plated in poly-L-lysine- (Sigma) and laminin (Invitrogen)-coated wells; and incubated at 37 °C in 7.5% CO_2. From these cultures, murine Schwann cells could be expanded for up to four passages, changing the medium every 3 days. MG132 (Calbiochem) was used at 50 μM.

cDNA Constructs and Transfection—pCB6-Ezrin-VSV G, Sch-VSV G, SchΔF118-VSV G, and SchΔ39–121-VSV G expression plasmids were described previously (22, 23). EzrinΔF102-VSV G and SchΔ81–121-VSV G were constructed in pCB6. pCW7 expressing Myc-tagged ubiquitin was described previously (24). Transfection of the LLC-PK1 cell line was performed by electroporation (22). Transient transfectants

* This work was supported by grants from Ligue Nationale contre le Cancer, Association pour la Recherche contre le Cancer (Grant ARC 5599 (to M. A.) and Grant ARC 5676 (to M. G.)) and United States Army Research Medical Research and Materiel Command Award DAMD17-00-1-0594 (to M. G.). The costs of publication of this article were defrayed in part by the payment of page charges. This article must therefore be hereby marked "*advertisement*" in accordance with 18 U.S.C. Section 1734 solely to indicate this fact.

§ Present address: Dept. of Cell Biology, Harvard Medical School, Boston, MA 02115-5730.

‖ To whom correspondence should be addressed. Fax: 33-1-42346377; E-mail: marpin@curie.fr.

[1] The abbreviations used are: NF2, neurofibromatosis type 2; Sch, schwannomin; FERM, protein 4.1/ezrin/radixin/moesin; DMEM, Dulbecco's modified Eagle's medium; FBS, fetal bovine serum; VSV G, vesicular stomatitis virus G protein; pAb, polyclonal antibody; mAb, monoclonal antibody.

were analyzed after 20 h. Pools of stable transfectants were selected in medium containing 0.7 mg/ml G418 (Invitrogen).

Extracts and Immunoblotting—Confluent cells in 3-cm dishes were washed once in cold phosphate-buffered saline, lysed with 100 μl of hot 1× SDS loading buffer (62.5 mM Tris, 2% SDS, 10% glycerol, 0.01% bromphenol blue, 5% 2-mercaptoethanol), and scraped. These viscous total extracts were then sonicated for 2 min in a bath sonicator (Branson Sonifier 250). Soluble extracts were prepared by a 1-min extraction in 100 μl of cold 50 mM Hepes, 150 mM NaCl, 10 mM EDTA, 1% Triton X-100, pH 7.4 and then supplemented with 3× SDS loading buffer. The insoluble fractions were then prepared as total extracts. Extracts were boiled for 2 min before SDS-PAGE. Proteins were transferred to nitrocellulose membranes (Schleicher & Schuell). The following antibodies were used for immunoblotting: VSV G pAb (1 μg/ml), P5D4 VSV G mAb (1:2000), 9E10 Myc mAb (1 μg/ml), p75 nerve growth factor receptor pAb (1:200, Chemicon), Sch A19 pAb (1 μg/ml, Santa Cruz Biotechnology), ezrin pAb (1 μg/ml) (22).

Immunoprecipitation and Pull-down—To prepare lysates, cells were rinsed once with cold phosphate-buffered saline and extracted with cold RIPA buffer (50 mM Hepes, 150 mM NaCl, 10 mM EDTA, 1% Nonidet P-40, 0.5% sodium deoxycholate, 0.1% SDS, pH 7.4) supplemented with protease inhibitors (Sigma) for 2 min at 4 °C. The extracts were then clarified at 20,000 × g for 10 min at 4 °C. Denatured lysates were obtained by adding 500 μl of boiling 10 mM Hepes, 150 mM NaCl, 1% SDS, pH 7.4 and scraping. The lysates were boiled for 2 min. RIPA was then reconstituted with 4.5 ml of cold 54.4 mM Hepes, 150 mM NaCl, 11 mM EDTA, 1.1% Nonidet P-40, 0.56% sodium deoxycholate, pH 7.4. The extracts were clarified by centrifugation at 4000 rpm for 10 min. For immunoprecipitations, lysates were incubated with 10 μl of protein A-Sepharose (Amersham Biosciences) and 2 μg of VSV G pAb for LLC-PK1 transfectants or 5 μg of Sch A19 pAb for embryonic fibroblasts at 4 °C for 2 h or overnight for volumes larger than 1 ml. For the Ni^{2+} bead pull-down, transfected cells were extracted in 10 mM Tris-HCl, 100 mM NaH_2PO_4, 8 M urea, pH 8.0. The extracts were incubated with 20 μl of Ni^{2+} beads (Qiagen) for 2 h. The beads were washed four times with 10 mM Tris-HCl, 100 mM NaH_2PO_4, 8 M urea, pH 6.3.

Precipitated proteins were eluted by boiling for 2 min in 20 μl of 1.5× SDS loading buffer. The ^{35}S signal was enhanced by incubating gels in 1 M salicylate for 20 min. Dried gels were exposed to films at −80 °C or to a phosphoscreen from 1 day to 1 week.

Pulse-Chase Analysis—Metabolic labeling was achieved with 250 μCi/ml ^{35}S-labeled Met and Cys from Redivue Promix (Amersham Biosciences). LLC-PK1 and primary Schwann cells in 6-cm dishes or confluent primary mouse embryo fibroblasts in 150-cm^2 flasks were labeled for 15 min and chased for the indicated time in standard DMEM containing 10% FBS. After immunoprecipitation and SDS-PAGE, signals were quantified using a STORM 860 PhosphorImager and ImageQuant software (Amersham Biosciences). Only experiments in which an exponential decay regression ($y = a \times e^{-bx}$, where y is percentage of the $t = 0$ signal and x is time in hours, calculated with Microsoft Excel) gave a correlation coefficient $R^2 > 0.95$ were taken into account to calculate the half-life according to the formula: $t_{1/2} = (\ln(50) - \ln(a))/-b$. This procedure gave less than 10% variation between experiments.

RESULTS

SchΔF118 Is Efficiently Degraded by the Ubiquitin-Proteasome Pathway—To study the consequence of misfolding of the FERM domain on the stability of Sch, we expressed wild type Sch or SchΔF118 in LLC-PK1 cells. For comparison, we also expressed wild type ezrin and the equivalent mutant ezrin, ezrinΔF102. These exogenous proteins were tagged at their carboxyl terminus with a VSV G epitope. We derived pools of stable transfectants expressing these proteins. In a first attempt to study the stability of the ΔF proteins, we examined the effect of inhibiting proteasomes in these cells. The treatment for 6 h with MG132, a specific inhibitor of proteasomes, revealed a ladder of SchΔF bands by VSV G immunoblotting (Fig. 1*A*). This ladder is characteristic of polyubiquitylated proteins. For wild type Sch, an additional band with an up-shift of about 6 kDa was also revealed upon MG132 treatment. This band might correspond to the conjugation of one ubiquitin. A ladder of ezrinΔF was not detected when proteasomes were inhibited for 6 h. Since misfolded proteins tend to aggregate, we examined the solubility of SchΔF in 1% Triton X-100. When

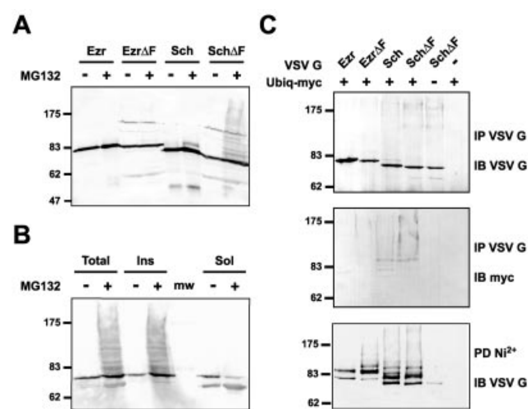

FIG. 1. **Ubiquitylation of SchΔF.** *A*, stable LLC-PK1 transfectants expressing wild type or mutant ezrin (*Ezr*) or Sch were subjected, or not, to MG132 for 6 h. Total lysates were immunoblotted with VSV G pAb. More lysate from cells expressing mutant proteins was loaded to give roughly equivalent signals with wild type and mutant proteins. This explains why some nonspecific bands appeared with those lysates. *B*, same experiment as in *A* except that SchΔF cells were extracted with a buffer containing 1% Triton-X100. The immunoblot was performed with VSV G pAb. *C*, cotransfection of wild type or mutant ezrin (*Ezr*) or Sch with a His_6- and Myc-tagged ubiquitin in LLC-PK1 cells. Immunoprecipitations (*IP*) of VSV G-tagged proteins was followed by VSV G or Myc immunoblotting (*IB*). Alternatively, ubiquitylated proteins were first precipitated in a pull-down (*PD*) experiment using Ni^{2+} beads and immunoblotted with VSV G antibodies. Note the low level of contaminating unmodified ezrin or Sch due to nonspecific binding of the overexpressed proteins to Ni^{2+} beads. Both experiments revealed that the high molecular weight smear of SchΔF corresponds to ubiquitylated material. *Ins*, insoluble; *Sol*, soluble; *Ubiq*, ubiquitin; *mw*, molecular weight markers.

proteasomes were inhibited, the amount of insoluble SchΔF increased, and interestingly, the ladder of putatively polyubiquitylated SchΔF was found to be completely insoluble (Fig. 1*B*).

To demonstrate that the ladder of SchΔF was due to ubiquitylation, we cotransfected cDNAs encoding His_6- and Myc-tagged ubiquitin and the various VSV G-tagged ezrin or Sch constructs. An extract was prepared from the transfected cells under denaturing conditions to inactivate ubiquitin hydrolases and to extract insoluble material. This extract was immunoprecipitated with VSV G antibodies, and the immunoprecipitates were probed with either VSV G antibodies or Myc antibodies. The VSV G immunoblot revealed the transfected proteins at their expected size (Fig. 1*C*). In addition, a weak smear of high molecular weight SchΔF was detected. This shifted material was also recognized by Myc antibodies, indicating that it corresponded to ubiquitylated SchΔF. In this assay, the ubiquitylated material produced a smear rather than a ladder, probably because of the coexistence of ubiquitin and tagged ubiquitin in transfected cells. We found that the converse experiment, the precipitation of ubiquitylated proteins with Ni^{2+} beads followed by a VSV G immunoblot (Fig. 1*C*), was more sensitive to detect the smear of ubiquitylated SchΔF. In contrast to the MG132 experiment on stable transfectants, ubiquitylation of Sch and ezrinΔF was also detected in this transient transfection system. We concluded that a low amount of SchΔF is polyubiquitylated at steady state. This polyubiquitylation explains the ladder of conjugates observed when proteasomes were inhibited.

Since polyubiquitylation tags proteins for degradation by proteasomes (25), we then evaluated the effect of the ΔF mutation on the stability of ezrin and Sch. The stability of the exogenous proteins from stable transfectants was analyzed by pulse-chase experiments. Cells were metabolically labeled with [^{35}S]methionine and chased for various times, and the exogenous proteins were immunoprecipitated with VSV G antibodies

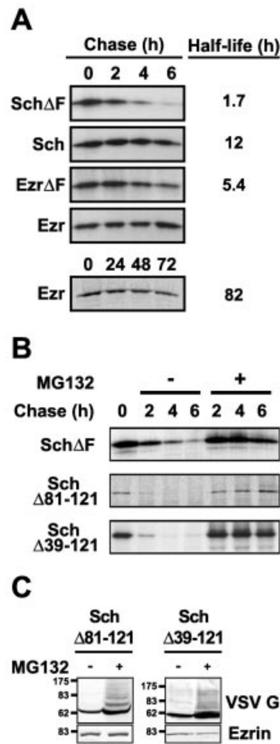

FIG. 2. **Pulse-chase analysis of mutant forms of Sch.** *A*, stable LLC-PK1 transfectants expressing wild type or mutant ezrin (*Ezr*) or Sch were pulse-labeled with ^{35}S for 15 min and chased for 0, 2, 4, or 6 h or chased for up to 72 h as indicated. VSV G immunoprecipitates were autoradiographed after SDS-PAGE. *B*, effect of MG132 on the stability of mutant Sch. SchΔF, SchΔ81–121, or SchΔ39–121 stable transfectants were treated, or not, with MG132 during the chase. VSV G immunoprecipitation was performed with denatured lysates to extract the MG132-induced insoluble pool. Inhibition of proteasomes blocks the efficient degradation of mutant Sch. *C*, SchΔ81–121 or SchΔ39–121 stable transfectants were subjected, or not, to MG132 for 6 h. Total lysates were immunoblotted with VSV G pAb. High molecular weight conjugates of SchΔ81–121 or SchΔ39–121 accumulate upon inhibition of proteasomes.

(Fig. 2*A*). We found SchΔF to be the most efficiently degraded protein with a half-life of less than 2 h. However, the ΔF mutation destabilized both Sch and ezrin (7-fold for Sch and 15-fold for ezrin). In wild type as well as mutant forms, Sch was less stable than ezrin (7-fold for wild type and 3-fold for mutant). To determine the role of proteasomes in the instability of SchΔF, we investigated the effects of MG132. Since treatment with MG132 produced insoluble SchΔF, we analyzed the total fraction using denatured extracts. The addition of MG132 during the chase greatly stabilized SchΔF, suggesting that this ubiquitylated protein is degraded by proteasomes (Fig. 2*B*). We sought to generalize this result to other mutant products. SchΔ81–121 and SchΔ39–121 are two deletions affecting the FERM domain. In stable transfectants, these two mutants proteins were also rapidly degraded by proteasomes with a half-life of 1 h for SchΔ81–121 and 0.6 h for SchΔ39–121 (Fig. 2*B*). In addition, SchΔ81–121 and SchΔ39–121 accumulated as high molecular weight conjugates upon inhibition of proteasomes (Fig. 2*C*) like SchΔF (Fig. 1*A*).

Endogenous SchΔ81–121 but Not Wild Type Sch Is Unstable in Primary Fibroblasts—To demonstrate that the instability of mutant Sch compared with wild type was not due to overexpression, we used primary embryonic fibroblasts derived from *Nf2* knock-out mice. Since the homozygous *Nf2* knock-out mice die too early in their embryonic development to derive fibroblasts (26), we analyzed mutant and wild type Sch expressed in a heterozygous $Nf2^{KO3/+}$ knock-out mouse (17). The $Nf2^{KO3}$ allele in which exon 3 is deleted encodes SchΔ81–121. We derived embryonic fibroblasts from this mouse and analyzed the stability of both wild type Sch and SchΔ81–121 through a pulse-chase experiment followed by immunoprecipitation with antibodies recognizing both forms. Wild type Sch was stable during the 6-h chase, but the SchΔ81–121 signal completely disappeared after a 2-h chase (Fig. 3*A*). At zero time, the SchΔ81–121 signal was about 40% that of Sch wild type. Since the two alleles are equally transcribed (17), this suggests that about 60% of SchΔ81–121 would have already been degraded during the pulse incubation of 15 min and consequently that the half-life of this endogenous mutant Sch would be less than 15 min. SchΔ81–121 was stabilized when MG132 was added

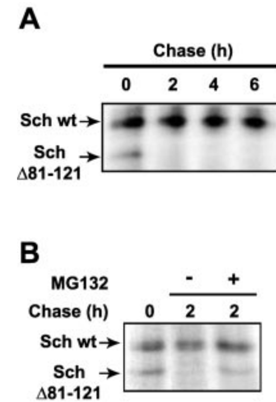

FIG. 3. **Pulse-chase analysis of an endogenous mutant Sch expressed in primary embryonic fibroblasts derived from an $Nf2^{KO3/+}$ heterozygous mouse.** *A*, the mutant Sch lacking amino acids encoded by exon 3 (SchΔ81–121), but not the wild type protein, is highly unstable. *B*, SchΔ81–121 is degraded by proteasomes. *wt*, wild type.

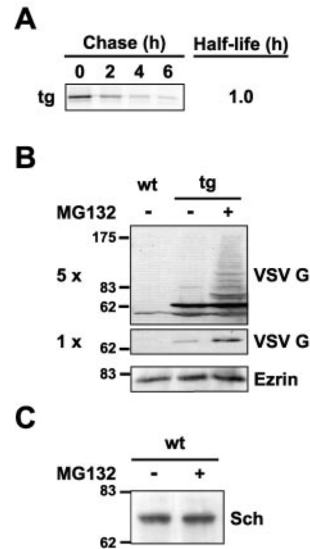

FIG. 4. **Instability of SchΔ39–121 in primary Schwann cells.** Primary cultures of Schwann cells from sciatic nerves were derived from wild type (*wt*) or transgenic (*tg*) mice expressing SchΔ39–121. *A*, primary cultures of Schwann cells derived from transgenic mice were pulse-labeled with ^{35}S for 15 min and chased for 0, 2, 4, or 6 h. VSV G immunoprecipitates were autoradiographed after SDS-PAGE. *B*, Schwann cell cultures were treated with MG132 for 6 h or were left untreated. Total extracts were immunoblotted with VSV G antibodies to detect tagged SchΔ39–121 or with ezrin antibodies as a loading control. SchΔ39–121 is stabilized when proteasomes are inhibited. In addition, when a 5-fold larger amount is loaded, a ubiquitin ladder of SchΔ39–121 becomes apparent. *C*, the level of endogenous Sch in wild type Schwann cells is not affected by the same MG132 treatment.

during the chase (Fig. 3*B*), indicating that its degradation is mediated by proteasomes.

SchΔ39–121 Is Unstable in Primary Schwann Cells—To examine whether this degradation pathway for mutant Sch is also functional in Schwann cells, the primary NF2-affected lineage, we used transgenic mice expressing SchΔ39–121 under the control of the Schwann-specific P0 promoter. These mice have been shown to develop schwannomas (16). We derived primary Schwann cells from sciatic nerves of these transgenic and wild type mice. These cultures contained >90% of Schwann cells as assessed by nerve growth factor receptor (p75) immunoreactivity (data not shown) (27). A pulse-chase experiment followed by immunoprecipitation with anti-VSV-G antibodies indicated that SchΔ39–121 has a half-life of 1 h (Fig. 4*A*). Consistently, an extract treated with MG132 for 6 h displayed a drastically enhanced level of SchΔ39–121 (Fig. 3*B*). When 5-fold more extract was loaded, a ubiquitin ladder of SchΔ39–121 became apparent in the MG132-treated extract (Fig. 4*B*). Consequently, SchΔ39–121 is likely degraded by the ubiquitin-proteasome pathway in primary Schwann cells. In contrast, endogenous Sch in wild type Schwann cells was not affected by the same MG132 treatment (Fig. 4*C*).

DISCUSSION

We have studied some pathogenetic mutations of the *NF2* tumor suppressor gene. The ΔF118, Δ81–121, and Δ39–121 mutations impair the proper folding of the Sch FERM domain as evidenced by chymotryptic digestions (7). The ΔF mutation in the FERM domain significantly destabilized both Sch and ezrin. However, SchΔF displayed a half-life of less than 2 h, 3-fold shorter than that of ezrinΔF. This difference might reflect the difference in stability of the wild type proteins, wild type Sch being less stable than wild type ezrin. At steady state, SchΔF was found to be ubiquitylated. Furthermore, when proteasomes were inhibited, a ubiquitin ladder was revealed, and SchΔF degradation was inhibited. We generalized these observations to SchΔ81–121 and SchΔ39–121. These three mutant forms of Sch are thus degraded by the ubiquitin-proteasome pathway. The efficient degradation of mutant Sch is not an artifact of overexpression since the degradation of endogenous SchΔ81–121 in primary fibroblasts derived from *Nf2* knock-out mice was even more efficient than in stable transfectants. This result explains why this mutant Sch is hardly detected compared with the wild type Sch in heterozygous *Nf2* knock-out mice although the two alleles are equally transcribed (17). Wild type Sch was also found to be ubiquitylated when overexpressed. However, in primary Schwann cells, the level of endogenous Sch is not increased by inhibition of proteasomes, suggesting that this tumor suppressor protein is not primarily regulated through its degradation.

In human tumors, biallelic inactivation of the *NF2* gene is observed, and mutant proteins are undetectable (12–15). In contrast, transgenic mice expressing SchΔ39–121 in Schwann cells develop schwannomas in a dominant oncogenic manner (16). The mechanism by which overexpressed mutant Sch has a dominant effect on cell growth is not known. We derived primary cultures of Schwann cells from these transgenic mice and found that SchΔ39–121 is degraded by the ubiquitin-proteasome pathway since this mutant Sch was stabilized and accumulated in its ubiquitylated form when proteasomes were inhibited. Thus, the degradation of mutant forms of Sch by the ubiquitin-proteasome system reported herein is a functional pathway in Schwann cells, the primary NF2-affected lineage. In addition, in the sciatic nerves of these transgenic mice, the level of SchΔ39–121 was found to be similar to that of the endogenous wild type Sch (16). To display this amount of SchΔ39–121, a high level of overexpression must overcome proteasome-mediated degradation in this model. This situation contrasts with the low level of mutant Sch in human tumors. Taken together these observations strongly argue that dominant oncogenic effects observed with mutant Sch are due to overexpression and that they are not observed at a physiological level of expression because of the efficient degradation of mutant Sch.

This study establishes the importance of the ubiquitin-proteasome pathway in degrading potentially dominant, misfolded, mutant products of the *NF2* tumor suppressor gene. Such a mechanism might be at the core of tumor suppressor/oncogene distinction. In fact, without this efficient degradation pathway, one mutation creating a dominant protein such as SchΔ39–121 would be sufficient to produce schwannomas, and the *NF2* gene would behave as an oncogene rather than a tumor suppressor gene.

Acknowledgments—We thank Dr. N. Ratner for invaluable advice on murine Schwann cell culture, Drs. L. Goutebroze and R. Kopito for gifts of plasmids, and Drs. J. Kyte, J. Plastino, N. Ayad, and O. Stemmann for critical reading of the manuscript.

REFERENCES

1. Gusella, J. F., Ramesh, V., MacCollin, M., and Jacoby, L. B. (1999) *Biochim. Biophys. Acta* **1423,** 29–36
2. Rouleau, G. A., Merel, P., Lutchman, M., Sanson, M., Zucman, J., Marineau, C., Hoang-Xuan, K., Demczuk, S., Desmaze, C., Plougastel, B., Pulst, S. M., Lenoir, G., Bijlsma, E., Fashold, R., Dumanski, J., de Jong, P., Parry, D., Eldrige, R., Aurias, A., Delattre, O., and Thomas, G. (1993) *Nature* **363,** 515–521
3. Trofatter, J. A., MacCollin, M. M., Rutter, J. L., Murrell, J. R., Duyao, M. P., Parry, D. M., Eldridge, R., Kley, N., Menon, A. G., Pulaski, K. *et al.* (1993) *Cell* **72,** 791–800
4. Gutmann, D. H., Haipek, C. A., and Lu, K. H. (1999) *J. Neurosci. Res.* **58,** 706–716
5. Nguyen, R., Reczek, D., and Bretscher, A. (2001) *J. Biol. Chem.* **276,** 7621–7629
6. Sherman, L., Xu, H.-M., Geist, R. T., Saporito-Irwin, S., Howells, N., Ponta, H., Herrlich, P., and Gutmann, D. H. (1997) *Oncogene* **15,** 2505–2509
7. Brault, E., Gautreau, A., Lamarine, M., Callebaut, I., Thomas, G., and Goutebroze, L. (2001) *J. Cell Sci.* **114,** 1901–1912
8. Xu, H.-M., and Gutmann, D. H. (1998) *J. Neurosci. Res.* **51,** 403–415
9. Gutmann, D. H., Sherman, L., Seftor, L., Haipek, C., Lu, K. H., and Hendrix, M. (1999) *Hum. Mol. Genet.* **8,** 267–275
10. Shaw, R. J., Paez, J. G., Curto, M., Yaktine, A., Pruitt, W. M., Saotome, I., O'Bryan, J. P., Gupta, V., Ratner, N., Der, C. J., Jacks, T., and McClatchey, A. I. (2001) *Dev. Cell* **1,** 63–72
11. Morrison, H., Sherman, L. S., Legg, J., Banine, F., Isacke, C., Haipek, C. A., Gutmann, D. H., Ponta, H., and Herrlich, P. (2001) *Genes Dev.* **15,** 968–980
12. Deguen, B., Goutebroze, L., Giovannini, M., Boisson, C., Van der Neut, R., Jaurand, M.-C., and Thomas, G. (1998) *Int. J. Cancer* **77,** 554–560
13. Gutmann, D. H., Giordano, M. J., Fishback, A. S., and Guha, A. (1997) *Neurology* **49,** 267–270
14. Stemmer-Rachamimov, A. O., Xu, L., Gonzalez-Agosti, C., Burwick, J. A., Pinney, D., Beauchamp, R., Jacoby, L. B., Gusella, J. F., Ramesh, V., and Louis, D. N. (1997) *Am. J. Pathol.* **151,** 1649–1654
15. den Bakker, M. A., van Tilborg, A. A., Kros, J. M., and Zwarthoff, E. C. (2001) *Neuropathology* **21,** 168–173
16. Giovannini, M., Robanus-Maandag, E., Niwa-Kawakita, M., van der Valk, M., Woodruff, J. M., Goutebroze, L., Merel, P., Berns, A., and Thomas, G. (1999) *Genes Dev.* **13,** 978–986
17. Giovannini, M., Robanus-Maandag, E., van der Valk, M., Niwa-Kawakita, M., Abramowski, V., Goutebroze, L., Woodruff, J. M., Berns, A., and Thomas, G. (2000) *Genes Dev.* **14,** 1617–1630
18. Koga, H., Araki, N., Takeshima, H., Nishi, T., Hirota, T., Kimura, Y., Nakao, M., and Saya, H. (1998) *Oncogene* **17,** 801–810
19. Faudoa, R., Xue, Z., Lee, F., Baser, M. E., and Hung, G. (2000) *Hum. Mutat.* **15,** 474–478
20. Hogan, B., Beddington, R., Costantini, F., and Lacy, E. (1994) *Manipulating the Mouse Embryo: A Laboratory Manual*, 2nd Ed., Cold Spring Laboratory Press, Cold Spring Harbor, NY
21. Morrissey, T. K., Kleitman, N., and Bunge, R. P. (1991) *J. Neurosci.* **11,** 2433–2442
22. Gautreau, A., Louvard, D., and Arpin, M. (2000) *J. Cell Biol.* **150,** 193–203
23. Deguen, B., Mérel, P., Goutebroze, L., Giovannini, M., Reggio, H., Arpin, M., and Thomas, G. (1998) *Hum. Mol. Genet.* **7,** 217–226
24. Ward, C. L., Omura, S., and Kopito, R. R. (1995) *Cell* **83,** 121–127
25. Hershko, A., and Ciechanover, A. (1998) *Annu. Rev. Biochem.* **67,** 425–479
26. McClatchey, A. I., Saotome, I., Ramesh, V., Gusella, J. F., and Jacks, T. (1997) *Genes Dev.* **11,** 1253–1265
27. Pelton, P. D., Sherman, L. S., Rizvi, T. A., Marchionni, M. A., Wood, P., Friedman, R. A., and Ratner, N. (1998) *Oncogene* **17,** 2195–2209